GABAergic activation in the dorsal hippocampus in an acute pentylenetetrazol
seizure model in adult rats

by

Zoe Weiss

Claire-Anne Gutekunst
Adviser

Neuroscience and Behavioral Biology

Claire-Anne Gutekunst
Adviser

Kristen Frenzel
Committee Member

Dieter Jaeger
Committee Member

2016

GABAergic activation in the dorsal hippocampus in an acute pentylenetetrazol
seizure model in adult rats

By

Zoe Weiss

Claire-Anne Gutekunst
Adviser

An abstract of
a thesis submitted to the Faculty of Emory College of Arts and Sciences
of Emory University in partial fulfillment
of the requirements of the degree of
Bachelor of Sciences with Honors

Neuroscience and Behavioral Biology

2016

Abstract

GABAergic activation in the dorsal hippocampus in an acute pentylenetetrazol
seizure model in adult rats
By Zoe Weiss

The pattern of activation of GABAergic and parvalbumin (PV)-containing
interneurons over time was investigated in the dentate gyrus and CA3 region of the
dorsal hippocampus following pentylenetetrazol (PTZ)-induced seizures in adult
rats. Sections though the dorsal hippocampus were immunostaining for *c-fos*,
GAD67 and parvalbumin and colocalization analyzed using semi-quantitative cell
counts. Overall, the expression of *c-fos* in the dentate gyrus and CA3 increased over
time in the PTZ-treated animals. There was a significant difference between
activation of GABAergic interneurons of PTZ-treated animals and controls, however,
in both the dentate gyrus and CA3 GABAergic activation did not change over time.
Activation of PV-containing interneurons was significantly greater in PTZ-treated
animals compared to controls. However, the activation of PV-containing
interneurons changed in an unexpected time-dependent manner. In the dentate
gyrus, activation of PV-containing neurons was greatest at the earliest time point
from the onset of behavioral seizures, and in the CA3 activation was greatest at the
latest time point from the onset of behavioral seizures. At least 70% of activated
neurons in the hippocampus did not express PV or GAD67, thus a majority of the
activation during the induced seizures takes place in the glutamatergic neurons.
These data suggest that in an acute PTZ model, targeted inhibition of the
glutamatergic populations in the hippocampus would be more effective for limiting
seizure propagation.

GABAergic activation in the dorsal hippocampus in an acute pentylenetetrazol
seizure model in adult rats

By

Zoe Weiss

Claire-Anne Gutekunst
Adviser

A thesis submitted to the Faculty of Emory College of Arts and Sciences
of Emory University in partial fulfillment
of the requirements of the degree of
Bachelor of Sciences with Honors

Neuroscience and Behavioral Biology

2016

Table of Contents

Introduction

Epilepsy and its Current Treatments

An estimated 3 million individuals in the United States are burdened by the neurological

disorder, epilepsy (Kobau et al., 2012; Russ et al., 2012). Epilepsy is characterized by

recurrent, spontaneous seizures unprovoked by an acute systemic or neurologic insult

(Bromfield et al., 2006). These spontaneous seizures arise from the sudden and

temporary synchronization of neural activity, which occurs in response to an imbalance

between excitatory and inhibitory neurotransmission in the brain (Cloix and Hévor,

2009). Individuals with epilepsy deal with more than just unwanted seizures. A study

based on responses to the Behavioral Risk Factor Surveillance System (BFSS) found

individuals with active epilepsy to be more susceptible to comorbid illnesses, low

employment rates, and poor social relationships (Chong et al., 2010). This presents a high

demand for adequate treatments that can improve both the physiological symptoms and

the burdens on quality of life in epilepsy patients. The majority of epilepsy patients obtain

pharmacological treatment in the form of antiepileptic drugs (AEDs) (Sander, 2004).

These drugs work by altering the excitability of the neural networks through effects on

ion channels, neurotransmitter receptors or neurotransmitter metabolism (White et al.,

2007). AEDs, however, may come with a myriad of unwanted side effects such as

drowsiness, behavioral changes and weight gain (Kowski, 2016). About 70% of epilepsy

patients respond to AEDs, leaving one third of patients living with uncontrollable seizures

(Kwan and Brodie, 2000). Drug-resistant epilepsy patients have other surgical options

such as deep brain stimulation and hippocampal resection. However, these methods are

invasive and carry their own risks (Tykocki et al., 2012; Rohn et al., 2014). Thus, there is a

need for less invasive treatment strategies for drug-resistant epilepsy patients.

Optogenetics and Luminopsins

While promising treatments do exist, scientists have been exploring other possibilities

with more precision in the field of optogenetics. Optogenetics involves the use of light-

gated ion channels naturally produced bacteria to selectively regulate the activity of

specific populations of neurons, while leaving others unaffected (Bentley et al., 2013).

These channels, or opsins, regulate the flow of ions across the membrane of a cell in

response to specific wavelengths of light (Bentley et al., 2013). They can either lead to

depolarization or hyperpolarization, allowing for control of either excitation or inhibition

respectively (Kokaia et al., 2013). Optogenetics allows one to target the activity of specific

cell-type populations, an element lacking in other neural interface technology (Aravanis et

al., 2007).

The most common mode of light delivery for optogenetics in the brain is surgically

implanted, thin optical fibers coupled to an external bright light source (Zhang et al.,

2007). Successful modulation of behavior has been achieved with this method, however

challenges exist, such as potential for infection or tissue damage. In addition, differences

in the light scattering properties of different brain regions make it difficult to target

multiple structures with one fiber (Al-Juboori et al., 2013). One fiber can actually only

reach so many cells, creating a need for implantation of several LEDs to activate larger

structures, such as the hippocampus, thus increasing risk. As a way to overcome this

obstacle several laboratories, including ours, have coupled a bioluminescent light source

with an opsin, to degenerate luminopsins. These luminopsins can be either inhibitory

(iLMO2) or excitatory (LMO3) depending on the channel used in order to modulate

different neural circuitry (Berglund et al., 2016; Tung et al., 2015). iLMO2 combines

Renilla luciferase (RLuc), a bioluminescent protein, and *Natronomonas* halorhodopsin, a

light-driven chloride pump that hyperpolarizes the cell membrane (Tung et al., 2015).

Application of the RLuc substrate, coelenterazine (CTZ), to neurons expressing iLMO2

leads to production of bioluminescence and thus activation of the halorhodopsin (Tung et

al., 2015). iLMO2 suppressed single-unit firing rate and local field potential in the

hippocampus of anesthetized rats, demonstrating its capability to inhibit neural activity *in

vivo* (Tung et al., 2015). In contrast, LMO3 combines *Gaussia* luciferase with

channelrhodopsin in order to depolarize neuronal membranes and activate neurons

(Berglund et al., 2016). Application of CTZ to neurons expressing LMO3 in the substantia

nigra led to increased firing rate *in vivo* (Berglund et al., 2016). Thus, both iLMO2 and

LMO3 possess the potential to regulate epileptiform activity through modulation of

relevant cell populations.

The Hippocampus and Temporal Lobe Epilepsy

Human temporal lobe epilepsy (TLE) is characterized by spontaneous seizures that

originate focally and spread within the limbic system and beyond (Collins et al., 1983).

Alterations in several cell populations contribute to the development of TLE, especially in

the dentate gyrus of the hippocampus. The normal circuitry of the dentate gyrus involves

both feed-forward and feedback inhibition (Sloviter, 1991; Zipp et al., 1989). Projections

from the entorhinal cortex either directly innervate inhibitory interneurons, thus

inhibiting excitatory granule cells; or entorhinal projections can innervate the excitatory granule cells which activate interneurons that will inhibit granule cells (Bromfield et al., 2006). Experimental models of TLE have demonstrated mossy fiber sprouting within the dentate gyrus, increased excitability, and neuronal degeneration disrupt normal activity and give rise to seizures (Matzen et al., 2007; Sutula and Dudek, 2007).

The dentate gyrus has an essential role in seizure propagation. It acts as a filter that initially restricts the entry of seizures from the entorhinal cortex into the rest of the hippocampus (Heinemann et al., 1992). The granule cells have a relatively high activation potential, allowing for limitation of their response to synchronous activity (Fricke and Prince, 1984; Scharfman, 1992). Impairment of inhibition or enhanced excitation of the granule cells can cause the breakdown of this filter function and thus, an increase of hypersynchronous activity of dentate granule cells (Peng and Houser, 2005, Wittner et al., 2001).

Cell populations within the dentate gyrus include mostly glutamatergic and GABAergic neurons (Amaral et al., 2007; Houser, 2007) and these populations have distinct roles in carrying out the activity of the hippocampus. Two populations of principal glutamatergic cells reside in the dentate, hilar mossy cells and granule cells (Scharfman and Myers, 2013). The hilar mossy cells send excitatory projections to granule cells and GABAergic interneurons in the hilus as well (Ascády et al., 1998; Jackson and Scharfman, 1996). Evidence from human post-mortem tissue implicates loss of mossy cells as a characteristic of human TLE (Henze and Buzsáki, 2007). Two hypotheses have been proposed in regards to how mossy cell loss contributes to TLE. First, "the dormant basket cell" hypothesis holds that the degeneration of mossy cells removes excitatory

input to inhibitory basket cells, resulting in disinhibition of the granule cells (Slotviter, 1994; Sloviter et al., 2003). In contrast, the "irritable mossy cell" hypothesis proposes the remaining mossy cells have higher firing rates and enhance excitatory feedback to granule cells (Henze and Buzsáki, 2007). The dentate granule cells are more resistant to damage, and in TLE they sprout new axon collaterals, creating recurrent excitatory connections with other granule cells (Cronin, 1992; Maglóczky and Freund, 1993) GABAergic interneurons provide integral inhibitory inputs to granule and mossy cell networks that are often compromised in TLE (Amaral et al., 2007; Patrylo et al., 2000). A subpopulation of GABAergic neurons, present in the granule cell layer and hilus of the dentate, produces the calcium-binding protein parvalbumin (PV) (Kosaka et al., 1987). PV-containing interneurons provide powerful inhibitory input to granule cells and can control network excitability (Nitsch et al., 1990; Sesselo et al., 2015). Loss of these neurons in the hilus is often seen in human TLE (Buckmaster and Dudek, 1997). Other research has found increased amounts of PV-containing cells in the granule cell layer of affected brain tissue (Wittner et al., 2001). *In vivo* studies demonstrate that optogenetic activation of PV interneurons curtails spontaneous seizures (Krook-Magnuson et al., 2013; Paz). However other research suggests PV cell activation provokes seizure-like activity in the entorhinal cortex (Yekhlef et al., 2014). Wittner et al. (2001) indicate that increased excitability in the dentate granule cells in TLE could be due to loss of inhibition or more effective synchronization of granule cells due to alterations in PV neurons.

Pentylentetrazol Epilepsy Model and Cellular Activation

In the present study, we aimed to identify the hippocampal cell-types activated at the onset of acutely induced behavioral seizures to provide a better understanding of the pattern of activation during seizures. This information can later be used to target luminopsin expression in a cell type specific manner, and prevent the spread of seizures. We investigated this cell-type specific activation within the hippocampus using a pentylenetetrazol (PTZ) model of acute induced seizures in rats. PTZ is a chemical convulsant widely used in animal models of epilepsy and mimics the effects of generalized tonic-clonic seizures (Rubio et al., 2010). It is a known $GABA_A$ receptor antagonist that causes a loss of the inhibitory function of GABAergic neurons (Huang et al., 2001). Activation of neurons in response to PTZ-induced seizures can be examined using the immediate early gene, *c-fos,* since *c-fos* proto-oncogene levels increase rapidly in response to activation of nerve cells (Dragunow and Roberston, 1987). In a pilocarpine mouse model of TLE, *c-fos* labeling was observed in the dentate granule cells as early as 15 minutes from the onset of behavioral seizures. *C-fos* activation appeared in the different subtypes of GABAergic interneurons at later time points, including PV-containing GABAergic interneurons (Peng and Houser, 2005). Morgan et al. found increased *c-fos* mRNA levels in hippocampal neurons, with levels beginning to rise at 15 minutes after seizures induced by PTZ, and reaching a maximum 1 hour after the onset of seizures (Morgan et al., 1987). While studies have shown increases of *c-fos* expression in the hippocampus after acute PTZ-induced seizures, they do not investigate the patterns of activation in the specific cell-type populations for this particular model. We hypothesize that since the hippocampus contains populations of glutamatergic, GABAergic and

cholinergic neurons, the increase in *c-fos* or other immediate early genes might show a temporal pattern of activation during the propagation of seizures (Amaral et al., 2007; Frotscher et al., 1986; Yount et al., 1993). In the present study immunocytochemistry was used to evaluate activation, based on *c-fos* expression, of GABAergic interneurons and PV-containing interneurons over time throughout the dentate gyrus and CA3 pyramidal cell layer during the course of acute induced seizures.

Methods

Animals

Adult male Sprague-Dawley rats (200-250 grs) were obtained from Charles River (Wilmington, MA). All animals were maintained in a 12/12 light/dark cycle with *ad libitum* access to food and water. All protocols involving animals were approved by the Emory University Institutional Animal Care and Use Committee (IACUC) and conform to NIH guidelines. At the time of the experiments the rats weighed between 276-512 g.

Seizure Induction and Perfusion

In order to model acute induced seizures, rats in the experimental groups received an intraperitoneal injection of 60 mg/kg of PTZ. We initially injected 70 mg/kg, which resulted in a high mortality rate, thus we reduced the dose. The amount injected was determined by the weight of the rat. After the PTZ injection the rats' behavior was video recorded and observed for length and severity of seizures. We sacrificed each rat at one of

three different time points, 20, 40 or 80 minutes from the onset of behavioral seizures.

There were three rats used for each time point. Two control rats received saline and were

sacrificed 20 and 40 min from injection of saline. The control animal for 80 minutes

received a PTZ injection, however no seizure, or freezing was observed. Each adult rat

was deeply anesthetized with a lethal dose of Euthasol (130 mg/kg), injected

intraperitoneally, and then perfused intracardially with 0.9% NaCl, followed by 4%

paraformaldehyde in 0.1 M phosphate buffer at pH 7.2 (PB) for 15 min at a rate of 20 ml

per min. After perfusion the brains were removed from the skull and fixed for 1 hr in PF,

then cryprotected in 30% sucrose.

Immunocytochemistry

All collected brains were sectioned using a cryostat. Each brain was sectioned into 10 and

20 μm coronal sections collected on gelatin coated slides and 20 μm sections collected as

floating sections in 1% phosphate buffer solution (PBS). We collected sections at three

different antero-posterior levels (Level 1= Bregma -3.12 mm, Level 2= Bregma -3.96 mm,

Level 3= Bregma -4.68 mm based on other studies performed in the lab). Sections were

either collected on gelatin-coated slides (10 μm) and as floating sections (20 μm) in PBS

in 24 well trays. Immunocytochemistry was performed on the 10 μm sections

immediately after sectioning. Sections were warmed for 15 min on a slide warmer at 37°C

then a pap pen was used to draw boundaries around the sections. Sections were then

blocked with 4% donkey serum and 0.2% Triton X in PBS for 15 min at RT. The 20 μm

floating sections were rinsed in PBS for 10 min followed by blocking with 4% donkey

serum and 0.1% Triton X for 30 min. Rabbit anti-*c-fos* was used at a concentration of

1:100 as a marker of cell activation (sc52, Santa Cruz Biotechnology, Inc., Dallas TX).

GABAergic interneurons were identified using glutamate decarboxylase (anti-GAD67) at a

concentration of 1:250 (MAB5406, Millipore, Temacula, CA). Mouse anti-parvalbumin at a

concentration of 1:500 was used to stain a subtype of GABAergic cells (MAB1572,

Millipore, Temacula, CA). The sections were incubated in a combination of anti-*c-fos* and

one of the cell-type specific antibodies overnight. After incubation in primary antibody,

the sections were rinsed 3 times for 10 min in PBS, then stained with donkey anti-rabbit

AlexaFluor 594 (A21207, Life Technologies, Eugene, OR) and donkey anti mouse

AlexaFluro 488 (A21202, Invitrogen, Eugene, OR) conjugated secondary antibodies at a

concentration of 1:1000 for 1 hr . Sections were rinsed 3 times for 10 min in PBS and

mounted on slides and coverslipped using Vecta-Shield hard-set mounting medium with

DAPI nuclear stain (Vector Laboratories, Burlingame, CA).

Imaging

Brain sections were imaged using an inverted fluorescent microscope (Leica DM IRE2)

equipped with a QImaging CCD camera and Simple PCI Software. For each section,

several consecutive micrographs were captured so as cover the entire dentate gyrus and

CA3 region (5 to eight pictures per side). This was done on both the left and right sides of

the hippocampus. Using Adobe Photoshop® the pictures from each dentate gyrus were

merged using the photomerge function. The composite images were then used for

analysis.

Data Analysis

In order to analyze the immunoreactivity within the dentate gyrus the composite images were first divided into 6 groups: parvalbumin levels 1, 2 and 3, and GAD67 levels 1, 2, and 3. The names of each composite image were entered into Microsoft Excel and assigned a number randomly generated using the sorting function. Images were renamed using those assigned numbers so as to blind the counter. All cells in all sections were counted in a semi-quantitative manner to include: the number of *c-fos* positive cells, the number of cells positive for either GAD67 or parvalbumin, and the number of cells with colocalization of GAD67 or parvalbumin and *c-fos* within the dentate gyrus (Outer layer, granule cell layer and hilus) and the CA3 layer*.* Cell counts were done manually with the aid of the cell counter plug-in in the program FIJI. Only cells with nuclear *c-fos* were counted since *c-fos* is synthesized in the cytoplasm and upon activation, translocates into the nucleus. From the cell counts, cellular activation was determined by calculating the percentage of *c-fos* positive nuclei that expressed both *c-fos* and GAD67 or PV, or by calculating the percentage of GAD67 or PV positive neurons that expressed both *c-fos* and GAD67 or PV. For the statistical analysis we used a nonparametric Wilcoxon/Kruskal-Wallis Test (alpha=.05) and all pairs were compared using the Wilcoxon Method due to the differences in variances between the groups and the non-normal distribution of the data.

Results

PTZ induced seizures

A total of 32 rats were used in this study. Of those, 27 received PTZ injections and 5

received saline injections. Following PTZ injection, 14 of the rats experienced behavioral

seizures and survived, 7 experienced seizures and died of status, and 6 shown no

behavioral sign of seizure (Table 1). The typical seizure started approximately 1 min and

30 s from the time of injection. The seizures were characterized by myoclonic jerks

throughout the body and lasted about 3 min. The rats that survived the induced seizures

displayed normal and calm behavior after recovery from the seizure. We observed that

the environment and the state of the rat might have impacted the severity of the seizures.

Rats that struggled during the injection tended to have more severe seizures resulting in

death. The same was observed for rats in the rooms during the injection of another

animal. Changes were made in our protocol to minimize stress.

Seizure induced c-fos *expression*

Using immunocytochemistry we determined the difference in *c-fos* expression over time

in the dentate gyrus and CA3 of the dorsal rat hippocampus after acute, PTZ-induced

seizures. Little to no *c-fos* immunostaining was detected in the dentate gyrus (Figure 1A)

and CA3 (Figure 1B) of the control animals. In contrast *c-fos* immunostained neurons

were present in the dentate gyrus and the CA3 of all the PTZ-treated animals (Figure 1A

and B). In the dentate gyrus, *c-fos* positive neurons were present in the hilus, the outer

layer and within the granule cell layer. Of note, neurons of the 20 min animals expressed

mostly cytoplasmis *c-fos*, suggesting initiation of activation in those neurons (Figure 1A and B). At 40 min and 80 min there was an increase in the amount of nuclear *c-fos* in the dentate gyrus, with comparable intensity at both time points (Figure 1A). A similar trend was seen within the CA3 layer (Figure 1B).

According to semi-quantitative analysis, the average number of neurons expressing *c-fos*, increased in the dentate gyrus over time (Figure 2A). The average number of *c-fos* positive neurons at each time point was significantly greater than the controls ($p < .05$). The average number of *c-fos* positive nuclei of control animals was 0.6 ± 0.2 (Mean + SEM) compared to 14.9 ± 2.7, 55.0 ± 13.8, and 73.5 ± 12.5 at 20, 40 and 80 min following onset of seizure respectively (Figure 2A). The differences in average number of *c-fos* positive nuclei in the dentate gyrus at 80 min was also significantly greater than the average number at 20 min ($p < .05$).

An overall increase in *c-fos* expression over time was also found in the CA3 region of the dorsal hippocampus. The *c-fos* expression at each time point was significantly greater than the expression in controls ($p < .05$). Specifically, the average number nuclei expressing *c-fos* was 0.2 ± 0.1 in control animals and 2.3 ± 0.6, 3.5 ± 0.9 and 4.3 ± 0.5 at 20, 40 and 80 min post seizure onset respectively (Figure 2B). The change in *c-fos* expression from 20 min to 80 min in the CA3 was also statistically significant ($p < .05$).

Activation pattern in GABAergic Interneurons

Activation of the GABAergic interneurons within the dentate gyrus and CA3 layer of the hippocampus was determined by quantifying the colocalization of *c-fos* and GAD67 antibodies. GAD67 showed a similar pattern of expression in the dentate gyrus across the

control and treated groups (Figure 3 b, e, h and k). GAD67 positive neurons were present in the hilus, and the outer layer with a few cells also seen embedded in the granule cell layer (Figure 3 b, e, h and k). GA67 was mostly cytoplasmic with staining extending into processes.

The average number of GAD67 positive neurons within the dentate gyrus was similar amongst all groups; 15.7 ± 2.2 in controls, 8.8 ± 1.8 at 20 min, 13.9 ± 1.9 at 40 min, and 13.6 ± 1.8 at 80 min (Figure 5A). We found no statistically significant differences in GAD67 expression over time, which is consistent with our micrographs observation and confirms the binding of the antibody to our desired target protein.

In the dentate gyrus, the percent of c-fos neurons expressing GAD was significantly higher in all the PTZ-treated groups compared to controls (p<.05) with no colocalization detected in the control animals. The average percentage of *c-fos* positive cells colocalized with GAD67 in the dentate gyrus remained somewhat the same throughout all three time points with 13.9% ± 2.4% at 20 min, 12.1% ± 2.8% at 40 min, and 13.4% ±2.1% at 80 min (Figure 5B). The average percent of GAD67 positive neurons colocalized with *c-fos* was 30.4% ± 9.8% at 20 min, 38.1% ± 10.0% at 40 min, and 43.8% ± 5.9% at 80 min (Figure 5C). At all time points the average percent of activated GAD67 expressing neurons was significantly greater than controls (p<.05).

Expression of the GAD67 antibody in the CA3 was consistent amongst animals in all groups. The average number of GAD67 positive neurons was 2.4 ± 0.3 in controls, 1.5 ± 0.4 at 20 min, 2.6 ± 0.4 at 40 min, and 2.4 ± 0.5 at 80 min (Figure 5D). Similar to what was seen in the dentate gyrus, we found an overall difference in colocalization of GAD67 and *c-fos* expression in the CA3 between PTZ-treated animals and controls (p<.05). The

average percent of colocalized *c-fos* nuclei with GAD67 in the CA3 was 0 in the controls, 9.9% ± 4.3% at 20 min, 8.8% ± 3.7% at 40 min, and 22.6% ± 8.0% at 80 min (Figure 5E). None of the differences between each time point showed statistical significance. There was no significant difference in the amount of GAD67 positive neurons colocalized with *c-fos* in the CA3. No GAD67 positive neurons in the control animals expressed *c-fos*. The average percent of GAD67 positive neurons also expressing *c-fos* was 10.9% ± 3.9% at 20 min, 17.7% ± 8.1% at 40 min, and 30.1% ± 9.7% at 80 min (Figure 5F).

Activation pattern of parvalbumin-containing GABAergic Interneurons

Parvalbumin positive neurons were found in the dentate gyrus of all animals (Figure 6 b, e, h, and k). Staining was evident in neuronal cell bodies in the hilus, the outer layer and the granule cell layer and was mostly cytoplasmic.

There was a significant overall difference in the amount of PV positive neurons in the dentate gyrus. The average number of PV positive neurons was 5.7 ± 1.8 in controls, 14.2 ± 2.1 at 20 min, 5.8 ± 1.1 at 40 min, and 14.9 ± 2.0 at 80 min (Figure 8A). PV expression at 20 min and 80 min was significantly greater than expression in controls and expression at 40 min ($p < .05$).

Overall, there was a significant difference in the colocalization of *c-fos* and PV expression. The average percent of *c-fos* positive nuclei with PV was 5.5% ± 2.6% in controls, 28% ± 5.2% at 20 min, 6.8% ± 2.7% at 40 min, and 13.2% ± 2.9% at 80 min (Figure 8B). The average percent colocalization at 20 min and 80 min was significantly greater than controls ($p < .05$). In addition, we found that colocalization at 20 min was significantly greater than colocalization at both 40 min and 80 min ($p < .05$). The average

percent of PV positive neurons colocalized with *c-fos* was significantly greater in PTZ-treated animals than in controls, and colocalization at 80 min was significantly greater than at 20 min (p<.05). The average percent of PV positive neurons colocalized with *c-fos* was 1.0% ± 0.4% in controls animals, 25.5% ± 6.4% at 20 min, 37.2% ± 12.7% at 40 min, and 52.2% ± 3.9% at 80 min (Figure 8C).

PV expression within the CA3 layer remained relatively consistent across all groups, with no significant differences in the average number of PV positive neurons over time. The average number of PV positive neurons in the CA3 was 2.3 ± 0.7 in controls, 3.7 ± 0.5 at 20 min, 2.6 ± 0.5 at 40 min, and 4.4 ± 0.4 at 80 min (Figure 8D).

There was however, an overall significant difference in the colocalization of *c-fos* and PV expression (p<.05). Average percent of *c-fos* positive neurons colocalized with PV was 1.7% ± 1.2% in controls, 17.1% ± 5.9% at 20 min, 12.4% ± 5.6% at 40 min, and 39.6% ± 4.9% at 80 min (Figure 8E). The average percent colocalization at 20 min and 80 min was significantly greater than controls (p<.05). Furthermore, the average percent colocalization at 80 min was also significantly greater than average percent colocalization at 20 min and 40 min (p<.05). The average percent of PV positive neurons colocalized with *c-fos* was 2.3% ± 1.6% in controls, 11.5% ± 4.3% at 20 min, 28.4% ± 14.0% at 40 min, and 37.8% ± 4.6% at 80 min (Figure 8F). The colocalization of PV positive neurons with *c-fos* was significantly greater at 80 min than both colocalization in controls and at 20 min (p<.05).

Discussion

The present findings regarding the change in *c-fos* expression over time in the dorsal rat hippocampus are consistent with previous studies showing a time-dependent increase of *c-fos* expression following PTZ injection (Jensen et al., 1993; Morgan et al., 1987). In adult rats increased *c-fos* mRNA and protein levels were found to increase as early as 30 minutes post PTZ-induced seizure onset with maximum expression at 1 and 2 hr and returning to baseline at 6 hr (Barros et al., 2015).

The percent of activated neurons that are GAD67 positive is increased from control to 20 min after seizure onset but does not continue to increase over time thereafter. The data therefore suggests that activation of GABAergic interneurons in the dentate gyrus and CA3 layer is independent of time. When looking at the percent of GAD67 positive cells colocalized with *c-fos*, the same trend is observed. This constant activation of GABAergic neurons could arise because GABAergic neurons with cell bodies in the molecular layer of the dentate gyrus receive excitatory input directly from the perforant-pathway, and those with cell bodies in the hilus receive excitatory input from granule cells in the dentate gyrus itself (Houser, 2007). Both of these excitatory populations contribute to the progression of seizures. Since only about 13% of *c-fos* expression was found in GABAergic cells, most of the activation likely takes place in the glutamatergic populations, including hilar mossy cells and granule cells, which could lead to more activation of the GABAergic cells. The observed activation of GAD67 positive neurons could also result from direct disinhibition of GABAergic neurons caused by PTZ via $GABA_A$ receptors. Accordingly, an

immunocytochemical study revealed a high density of $GABA_A$ receptor subunits on the

surface of a population of GABAergic neurons in the dentate gyrus (Nusser et al., 1995).

Our results regarding the number of PV-containing interneurons in the

hippocampus are somewhat puzzling. We would expect no difference in the number of

PV-containing neurons between groups because PTZ treatment or time should not have

an effect on the number of neurons expressing PV based on the data for GAD67

expression. The number of PV containing neurons in the hippocampus has been shown to

decrease with age in Wistar over a period of 2 years, which is far from the time course of

our study (Lolova and Davidoff, 1992). Without further investigation, the inconsistencies

in the number between the various groups remain elusive. Since PV expression at 40 min

differs from that of the other time points, addition of 40 min animals would be one way to

investigate this further.

Within the dentate gyrus PV activation appears to be greater at the earliest time

point of 20 min, while in the CA3, PV activation is highest at the latest time point of 80

min. Strong excitatory input from the entorhinal cortex to PV interneurons in the dentate

gyrus could account for the early activation of these cells (Zipp et al., 1989). Our study

differs from previous findings in a spontaneous pilocarpine model of epilepsy showing

that recruitment of PV and GAD positive neurons occurs at 1 hr post-spontaneous seizure

(Peng and Houser, 2005). The differences could stem from the different mechanism of the

chemical convulsant used to induce the seizure. While PTZ works through $GABA_A$

receptors, pilocarpine is an agonist for muscarinic acetylecholine receptors (Rubio et el.,

2010). Alternatively, these discrepancies could be explained explanation by the distinct

seizure paradigm of each model. In a spontaneous pilocarpine model, the brain may

undergo physiological changes that contribute to occurrence of seizures, whereas in an acute PTZ model, seizures are a result of temporary changes in chemical transmission. Furthermore, it is to be noted that the results of the pilocarpine spontaneous study are not based on quantitative analysis but rather on qualitative co-localization in what appears to be a small region within the dentate gyrus. When looking at PV activation in terms of the percentage of PV positive cells colocalized with *c-fos* in the dentate gyrus and CA3 there is an increase from 20 min to 80 min. This way of analyzing the data accounts for the disproportionate increase of *c-fos* expressing neurons over time.

We conducted the present study in order to determine the cell-type specific pattern of activation in the hippocampus after acute, PTZ-induced seizures to potentially target relevant populations with inhibitory luminopsin and inhibit the spread of seizures within and from the hippocampus. Our data suggest, that in this particular model of epilepsy, activation within the dentate gyrus and CA3 seems to occur in both the glutamatergic and GABAergic neurons early on in the seizure, with a greater extent of activation in glutamatergic populations. Thus, targeting either glutamatergic populations, or targeting all cell-type populations of the hippocampus would be most effective in inhibiting the spread of seizures.

References

Al-luboori SI, Dondzillo A, Stubblefield EA, Felson G, Lei TC, Klug A (2013) Light
    scattering properties vary across different regions of the adult mouse brain. PLoS
    One 8:e67626.

Amaral DG, Scharfman HE, Lavenex P (2007) The dentate gyrus: fundamental
    neuroanatomical organization. Prog Brain Res 163:3-22.

Aravanis AM, Wang LP, Zhang F, Meltzer LA, Mogri MZ, Schneider MB, Deisseroth K
    (2007) An optical neural interface: in vivo control of rodent motor cortex with
    integrated fiberoptic and optogenetic technology. J Neural Eng 4:S143-156.

Acsady L, Kamondi A, Sik A, Freund T, Buzsaki G (1998) GABAergic cells are the major
    postsynaptic targets of mossy fibers in the rat hippocampus. J Neurosci 18:3386-
    3403.

Barros VN, Mundim M, Galindo LT, Bittencourt S, Porcionatto M, Mello LE (2015)
    The pattern of c-Fos expression and its refractory period in the brain of rats and
    monkeys. Front Cell Neurosci 9:72.

Bentley JN, Chestek C, Stacey WC, Patil PG (2013) Optogenetics in epilepsy.
    Neurosurg Focus 34:E4.

Berglund K, Birkner E, Augustine GJ, Hochgeschwender U (2013) Light-emitting
    channelrhodopsins for combined optogenetic and chemical-genetic control of
    neurons. PLoS One 8:e59759.

Bromfield EB, Cavazos JE, Sirven JI (2006) An introduction to epilepsy. Hartfor, CT:
    American Epilepsy Society. Chapter 1, Basic mechanisms underlying seizures and
    epilepsy. Available at: www.ncbi.nlm.nih.gov/books/nbk2510/.

Buckmaster PS, Dudek FE (1997) Network properties of the dentate gyrus in epileptic

    rats with hilar neuron loss and granule cell axon reorganization. J Neurophysiol

    77:2685-2696.

Chong J, Kudrimoti HS, Lopez DC, Labiner DM (2010) Behavioral risk factors among

    Arizonans with epilepsy: Behavioral Risk Factor Surveillance System 2005/2006.

    Epilepsy Behav 17:511-519.

Cloix J, Hévor T (2009) Epilepsy, regulation of brain energy metabolism and

    neurotransmission. Curr Med Chem 19:841-853.

Collins RC, Tearse RG, Lothman EW (1983) Functional anatomy of limbic seizures:

    focal discharges from medial entorhinal cortex in rat. Brain Res 280:25-40.

Cronin J, Obenaus A, Houser CR, Dudek FE (1992) Electrophysiology of dentate granule

    cells after kainate-induced synaptic reorganization of the mossy fibers. Brain Res

    573:305-310.

Dragunow M, Robertson HA (1987) Localization and induction of c-fos protein-like

    immunoreactive material in the nuclei of adult mammalian neurons. Brain Res

    440:252-260.

Fricke RA, Prince DA (1984) Electrophysiology of dentate gyrus granule cells. J

    Neurophysiol 51:195-209.

Frotscher M, Schlander M, Léránth C (1986) Cholinergic neuron in the hippocampus.

    A combined light- and electron- microscopic immunocytochemical study in the rat.

    Cell Tissue Res 246:293-301

Heinemann U, Beck H, Dreier JP, Ficker E, Stabel J, Zhang CL (1992) The dentate

gyrus as a regulated gate for the propagation of epileptiform activity. Epilepsy Res Suppl 7:273-280.

Houser CR (1990) Granule cell dispersion in the dentate gyrus of humans with temporal lobe epilepsy. Brain Res 535:195-204.

Henze DA, Buzsaki G (2007) Hilar mossy cells: functional identification and activity in vivo. Prog Brain Res 163:199-216.

Huang R, Bell-Horner CL, Dibas MI, Covey DF, Drewe JA, Dillon GH (2001) Pentylenetetrazol-induced inhibition of recombinant (gamma)-aminobutyric acid type A (GABA$_A$) receptors: mechanism and site of action. J Pharmacol Exp Ther 298:986-995.

Jackson MB, Scharfman HE (1996) Positive feedback from hilar mossy cells to granule cells in the dentate gyrus revealed by voltage-sensitive dye and microelectrode recording. J Neurophysiol 76:601-616.

Jensen FE, Firkusny IR, Mower GD (1993) Differences in c-fos immunoreactivity due to age and mode of seizure induction. Brain Res Mol Brain Res 17:185-193

Kobau R, Luo Y, PhD, Zack M, Helmers S, Thurman D (2012). Epilepsy in adults and access to care — United States, MMWR 61;909-913.

Kokaia M, Andersson M, Ledri M (2013) An optogenetic approach in epilepsy. Neuropharmocology 69:89-95.

Kosaka T, Katsumaru H, Hama K, Wu JY, Heizmann CW (1987) GABAergic neurons containing the Ca2+-binding protein parvalbumin in the rat hippocampus and dentate gyrus. Brain Res 419:119-130.

Kowski AB, Weissinger F, Gaus V, Fidzinski P, Losch F, Holtkamp M (2016) Specific

adverse effects of antiepileptic drugs - A true-to-life monotherapy study. Epilepsy

Behav 54:150-157.

Krook-Magnuson E, Armstrong C, Oijala M, Soltesz I (2013) On-demand optogenetic

control of spontaneous seizures in temporal lobe epilepsy. Nat Commun 4:1376.

Kwan P, Brodie MJ (2000) Early identification of refractory epilepsy. N Engl J Med

342:314-319.

Lolova I, Davidoff M (1992) Age-related morphological and morphometrical changes

in parvalbumin- and calbindin-immunoreactive neurons in the rat hippocampal

formation. Mech Ageing Dev 66:195-211.

Magloczky Z, Halasz P, Vajda J, Czirjak S, Freund TF (1997) Loss of Calbindin-D28K

immunoreactivity from dentate granule cells in human temporal lobe epilepsy.

Neuroscience 76:377-385.

Matzen J, Buchheim K, van Landeghem FK, Meierkord H, Holtkamp M (2008) Functional

and morphological changes in the dentate gyrus after experimental status

epilepticus. Seizure 17:76-83.

Morgan JI, Cohen DR, Hempstead JL, Curran T (1987) Mapping patterns of c-fos

expression in the central nervous system after seizure. Science 237:192-197.

Nitsch R, Soriano E, Frotscher M (1990) The parvalbumin-containing nonpyramidal

neurons in the rat hippocampus. Anat Embryol (Berl) 181:413-425.

Nusser Z, Roberts JD, Baude A, Richards JG, Sieghart W, Somogyi P (1995)

Immunocytochemical localization of the alpha 1 and beta 2/3 subunits of the

GABAA receptor in relation to specific GABAergic synapses in the dentate gyrus. Eur J Neurosci 7:630-646.

Patrylo PR, Spencer DD, Williamson A (2001) GABA uptake and heterotransport are impaired in the dentate gyrus of epileptic rats and humans with temporal lobe sclerosis. J Neurophysiol 85:1533-1542.

Peng Z, Houser CR (2005) Temporal patterns of Fos expression inf the dentate gyrus after spontaneous seizures in a mouse model of temporal lobe epilepsy. J Neuro 25:7210-7220.

Rohn B, Haenggi D, Etminan N, Kunz M, Turowski B, Steiger HJ (2014) Epilepsy, headache, and quality of life after resection of cerebral arteriovenous malformation. J Neurol Surg A Cent Eur Neurosurg 75:282-288.

Rubio C, Rubio-Osornio M, Retana-Márquez S, Verónica Custodio ML, Paz C (2010) *In vivo* experimental models of epilepsy. Cent Nerv Syst Agents Med Chem 10:298-309.

Russ SA, Larson K, Halfon N. (2012) A national profile of childhood epilepsy and seizure disorder. Pediatrics 129:256–64.

Sander JW (2004) The use of antiepileptic drugs- principles and practice. Epilepsia 45:28-34.

Scharfman HE (1992) Differentiation of rat dentate neurons by morphology and electrophysiology in hippocampal slices: granule cells, spiny hilar cells and aspiny 'fast-spiking' cells. Epilepsy Res Suppl 7:93-109.

Scharfman HE (1996) Hyperexcitability of entorhinal cortex and hippocampus after
    application of aminooxyacetic acid (AOAA) to layer III of the rat medial entorhinal
    cortex in vitro. J Neurophysiol 76:2986-3001.

Scharfman HE, Myers CE (2012) Hilar mossy cells of the dentate gyrus: a historical
    perspective. Front Neural Circuits 6:106.

Sessolo M, Marcon I, Bovetti S, Losi G, Cammarota M, Ratto GM, Fellin T, Carmignoto G
    (2015) Parvalbumin-Positive Inhibitory Interneurons Oppose Propagation But
    Favor Generation of Focal Epileptiform Activity. J Neurosci 35:9544-9557.

Sloviter RS (1991) Feedforward and feedback inhibition of hippocampal principal cell
    activity evoked by perforant path stimulation: GABA-mediated mechanisms that
    regulate excitability in vivo. Hippocampus 1:31-40.

Sloviter RS (1994) The functional organization of the hippocampal dentate gyrus and its
    relevance to the pathogenesis of temporal lobe epilepsy. Ann Neurol 35:640-654.

Sloviter RS, Zappone CA, Harvey BD, Bumanglag AV, Bender RA, Frotscher M (2003)
    "Dormant basket cell" hypothesis revisited: relative vulnerabilities of dentate
    gyrus mossy cells and inhibitory interneurons after hippocampal status epilepticus
    in the rat. J Comp Neurol 459:44-76.

Sutula TP, Dudek FE (2007) Unmasking recurrent excitation generated by mossy fiber
    sprouting in the epileptic dentate gyrus: an emergent property of a complex
    system. Prog Brain Res 163:541-563.

Tung JK, Gutekunst CA, Gross RE (2015) Inhibitory luminopsins: genetically
    encoded bioluminescent opsins for versatile, scalable, and hardware independent
    optogenetic inhibition. Nature

Tykocki T, Mondat T, Kornakiewicz A, Koziara H, Nauman P (2012) Deep brain
      Stimulation for refractory epilepsy. Arch Med Sci 8:805-816

White HS, Smith MD, Wilcox KS (2007) Mechanisms of action of antiepileptic drugs. Int
      Rev Neurobiol 81:85-110.

Wittner L, Magloczky Z, Borhegyi Z, Halasz P, Toth S, Eross L, Szabo Z, Freund TF (2001)
      Preservation of perisomatic inhibitory input of granule cells in the epileptic human
      dentate gyrus. Neuroscience 108:587-600.

Yekhlef L, Breschi GL, Lagostena L, Russo G, Taverna S (2015) Selective activation of
      parvalbumin- or somatostatin-expressing interneurons triggers epileptic
      seizurelike activity in mouse medial entorhinal cortex. J Neurophysiol 113:1616-
      1630.

Yount G, Ponsalle P, White JD (1993) Pentylenetetrazol-induced seizures stimulate
      transcription of early and late response genes. Mol Brain Res 21:219-224.

Zhang B, Wong M (2012) Pentylenetetrazol-induced seizures cause acute, but not
      chronic, mTOR pathway activation in rat. Epilepsia 53:506-511.

Zipp F, Nitsch R, Soriano E, Frotscher M (1989) Entorhinal fibers form synaptic contacts
      on parvalbumin-immunoreactive neurons in the rat fascia dentata. Brain Res
      495:161-166.

Figures and Tables

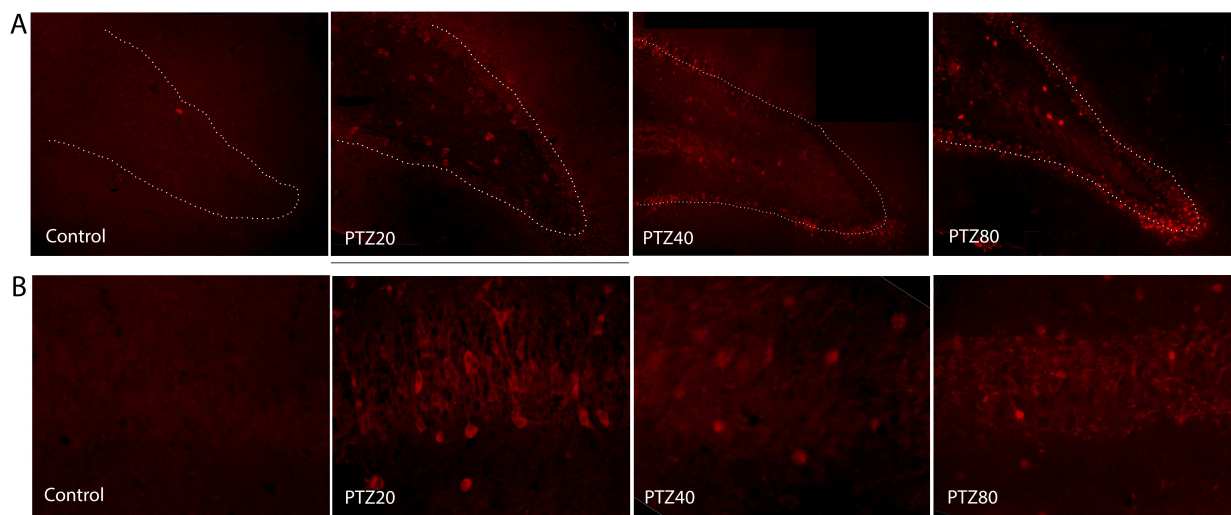| PTZ						Saline	
Seizure → Died	Seizure → Survived			No Seizure			
	20 min	40 min	80 min	40 min	80 min	20 min	40 min
7	4	7	3	3	3	1	4

Table 1.

Figure 1. A) Expression of *c-fos* (red) over time in the dentate gyrus. (scale bar: 300 µm)

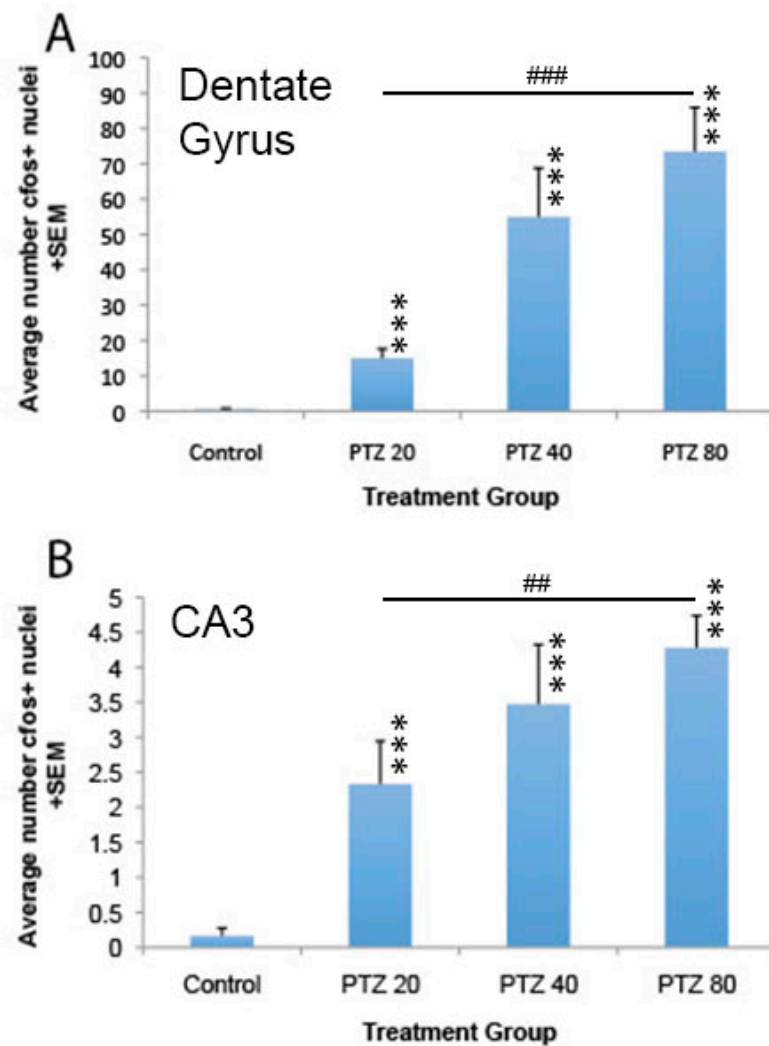B) Expression of *c-fos* (red) over time in the CA3 layer. (scale bar: 200 µm)

Figure 2. A) Time-dependent increase in *c-fos* expression in the dorsal rat dentate gyrus.

B) Time-dependent increase in *c-fos* expression in the dorsal rat CA3 layer. Animal

numbers were n=4 for controls, n=3 for all other groups. Statistics: *** p<.001 as
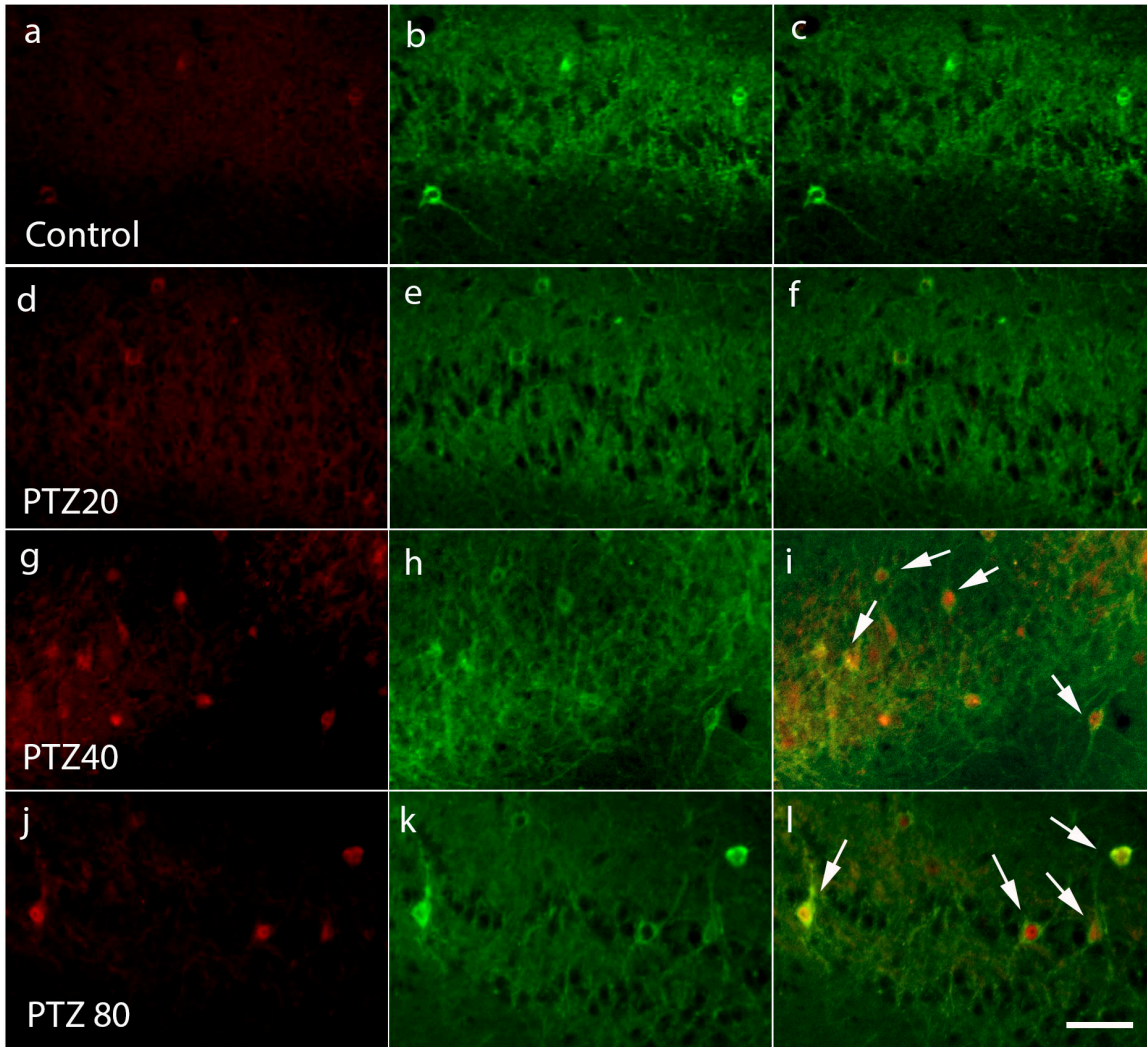
compared to controls; ## p<.01, ### p<.001 as indicated.
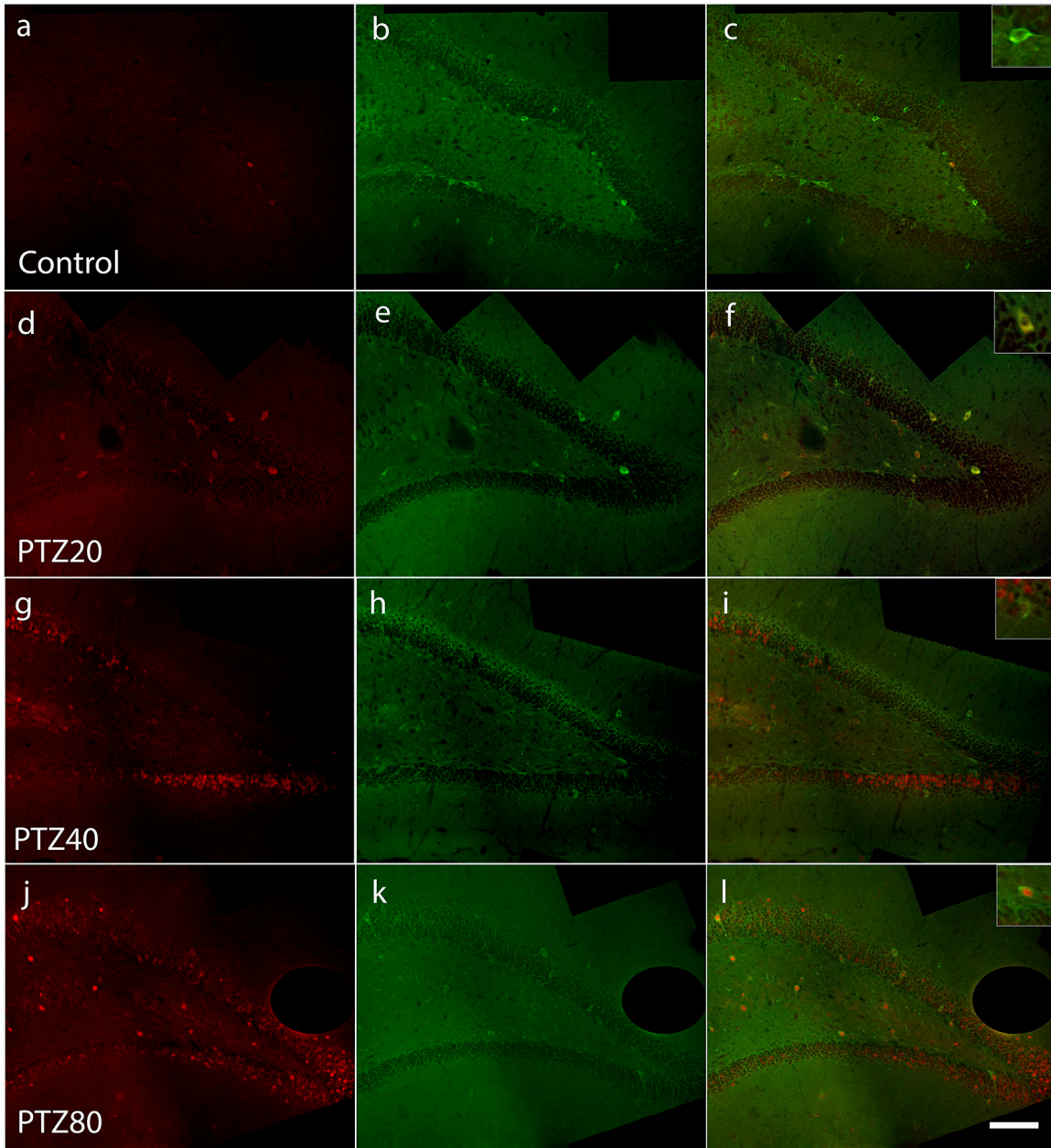
Figure 3. Expression of *c-fos* in red (a, d, g, j), GAD67 in green (b, e, h, k), and colocalization of *c-fos* and GAD67 (c, f, i, l) in the dentate gyrus of the dorsal hippocampus. (scale bar: 200 μm)

Figure 4. Expression of *c-fos* in red (a, d, g, j), GAD67 in green (b, e, h, k), and colocalization of *c-fos* and GAD67 (c, f, i, l) in the CA3 layer of the dorsal hippocampus. Arrows indicate colocalized cells in panels i and l. (scale bar: 100 μm)
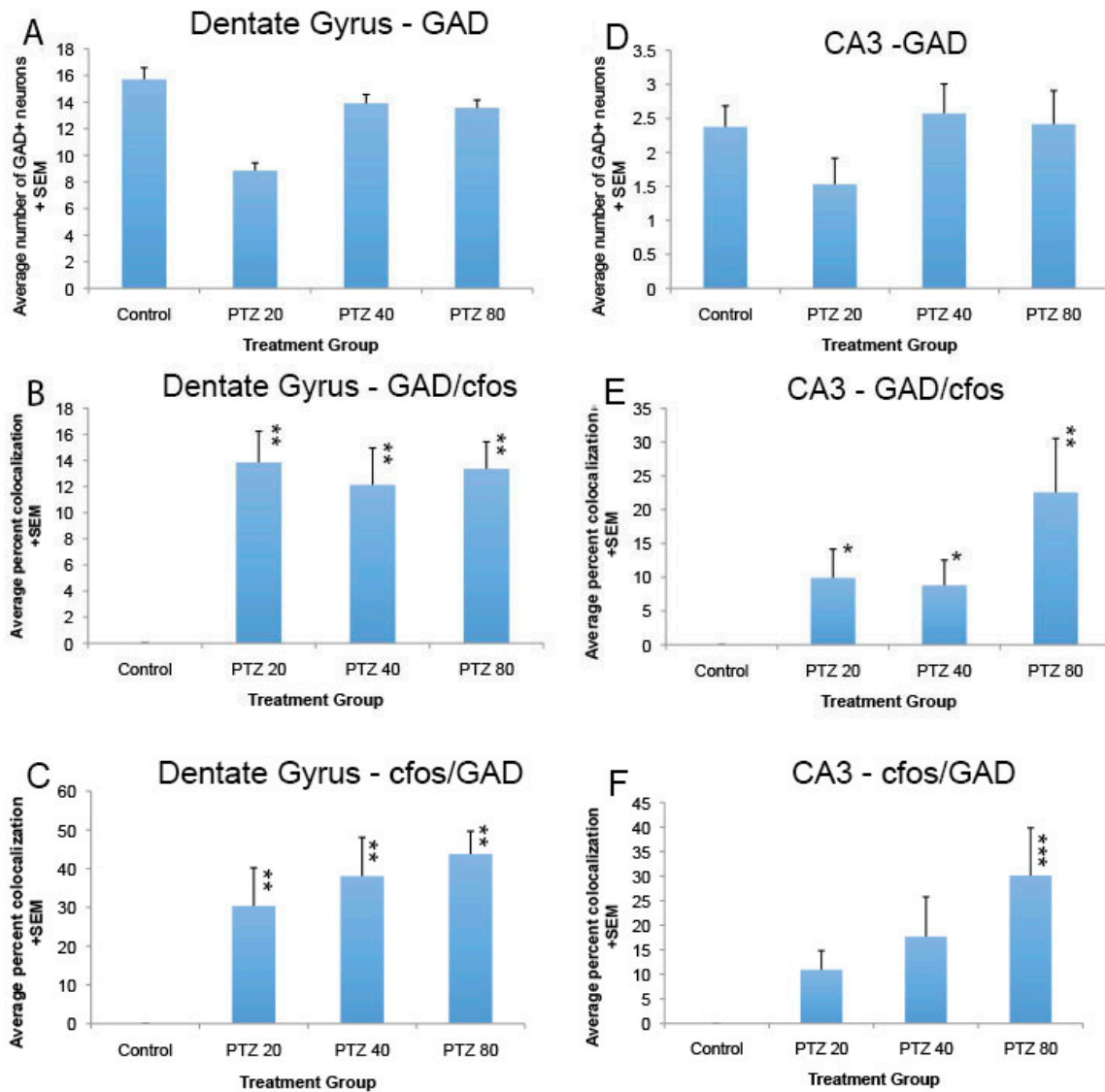
Figure 5. A) Overall expression of GAD67 in the dentate gyrus. B) Colocalization of *c-fos* positive nuclei with GAD67 in the dentate gyrus. C) Colocalization of GAD67 positive neurons with *c-fos* in the dentate gyrus. D) Overall expression of GAD67 in the CA3 layer. E) Colocalization of *c-fos* positive nuclei with GAD67 in the CA3 layer. F) Colocalization of GAD67 positive neurons with *c-fos* in the CA3 layer. Animal numbers were n=2 for controls, and n=3 for all other groups. Statistics: * p<.05, ** p<.01 as compared to controls.
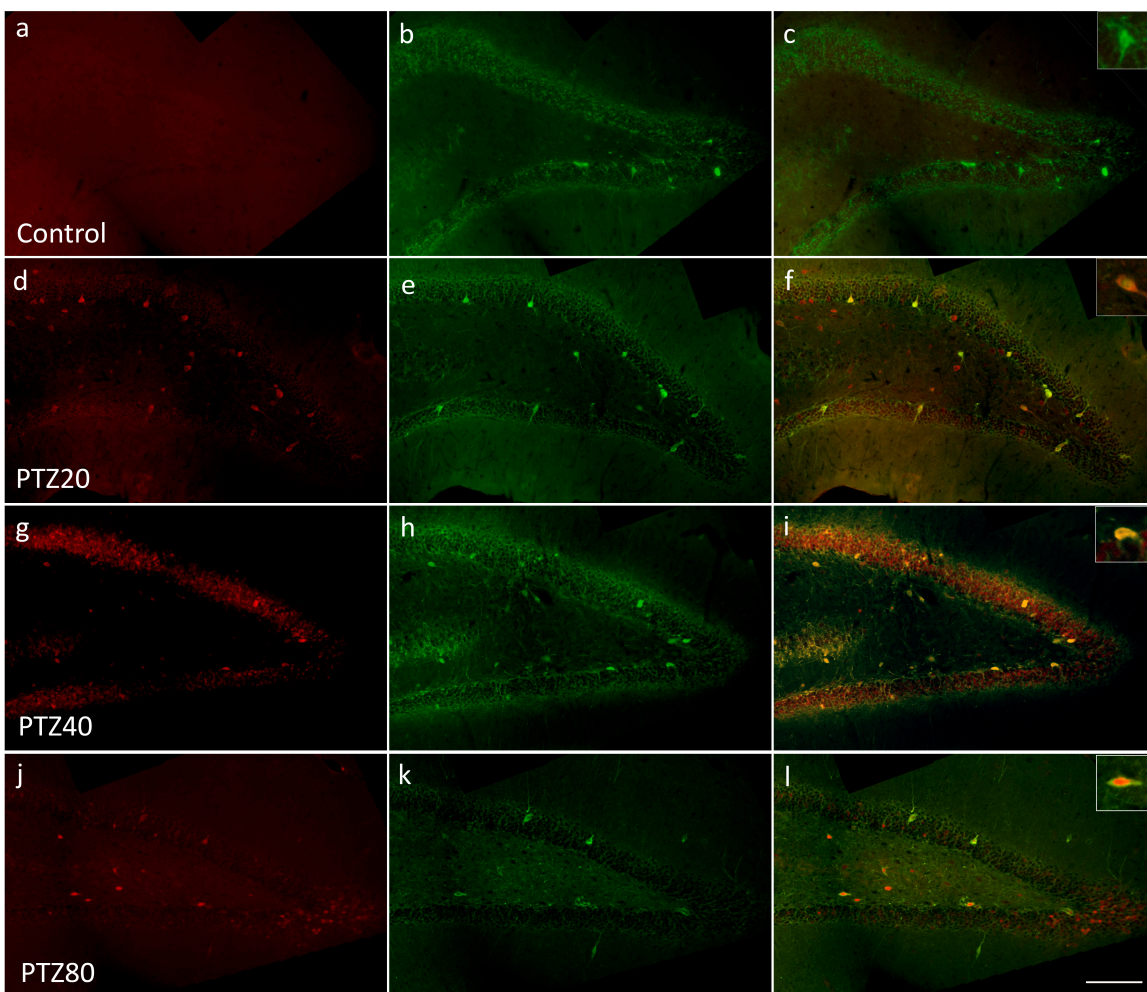
Figure 6. Expression of *c-fos* in red (a, d, g, j), parvalbumin in green (b, e, h, k), and colocalization of *c-fos* and parvalbumin (c, f, i, l) in the dentate gyrus of the dorsal hippocampus. (scale bar: 200 μm)
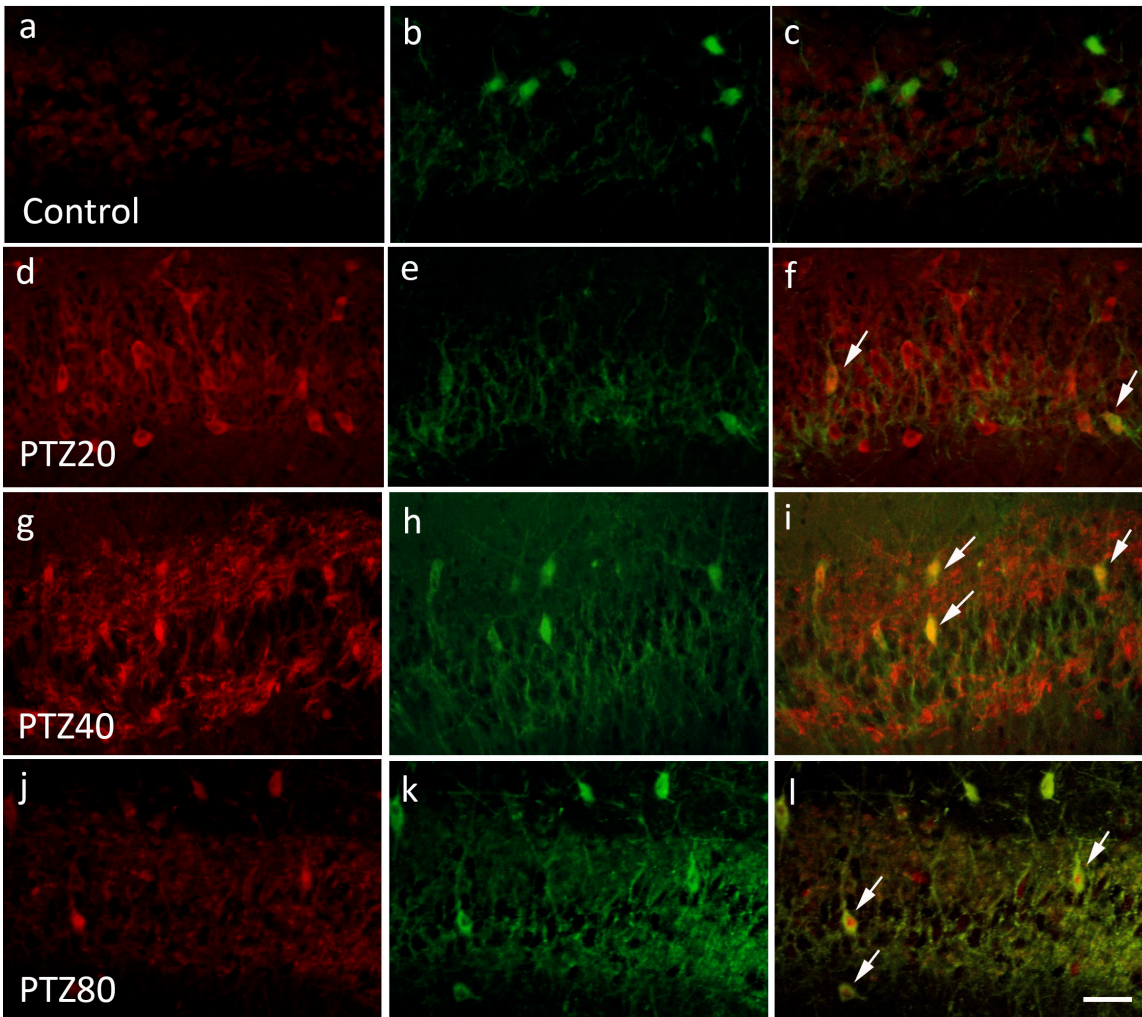
Figure 7. Expression of *c-fos* in red (a, d, g, j), parvalbumin in green (b, e, h, k), and colocalization of *c-fos* and parvalbumin (c, f, i, l) in the CA3 layer of the dorsal hippocampus. Arrows indicate colocalized cells in f, i, and l. (scale bar: 100 μm)
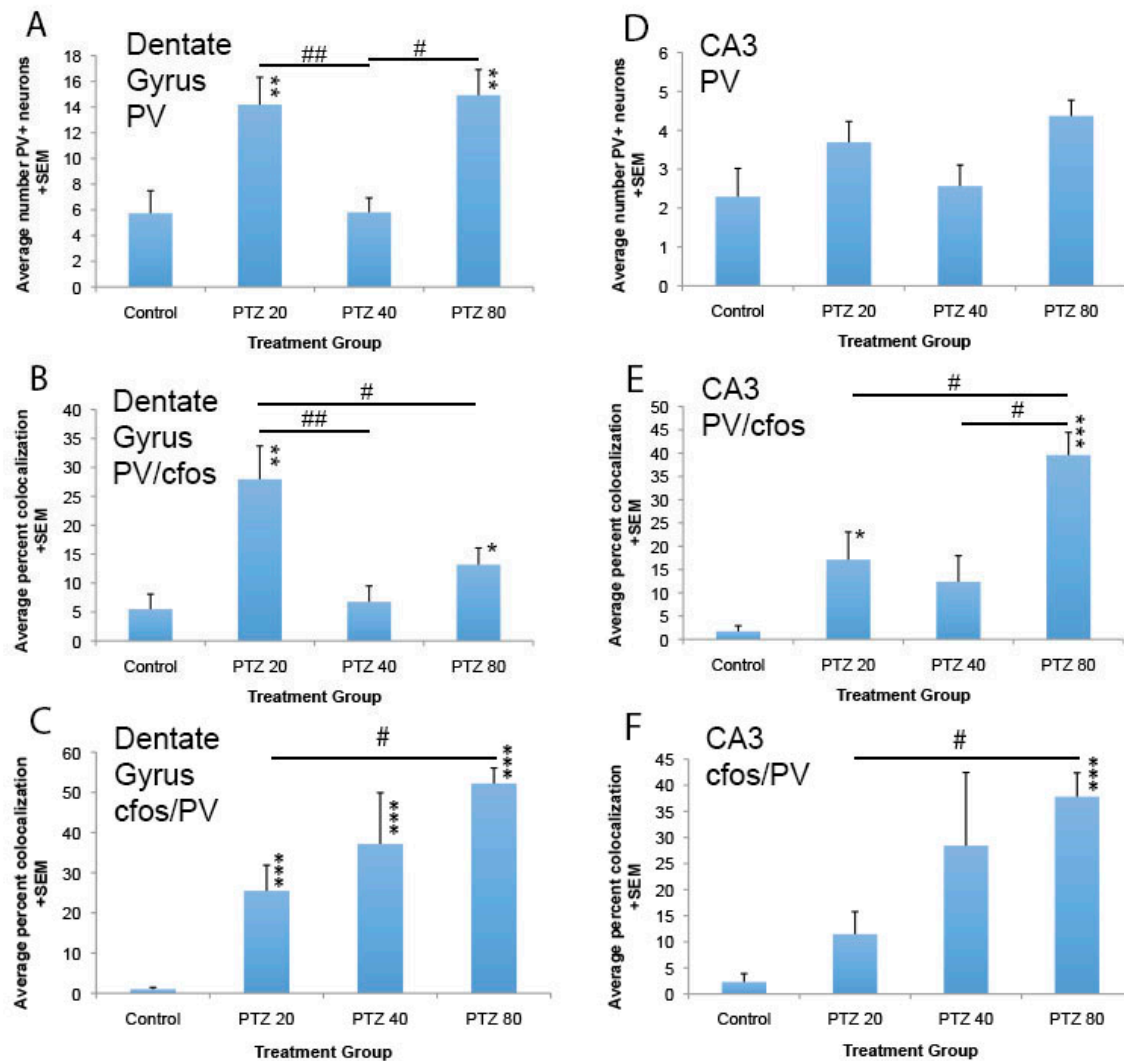
Figure 8. A) Overall expression of parvalbumin in the dentate gyrus. B) Colocalization of *c-fos* positive nuclei with paravalbumin in the dentate gyrus. C) Colocalization of parvalbumin positive neurons with *c-fos* in the dentate gyrus. D) Overall expression of parvalbumin in the CA3 layer. E) Colocalization of *c-fos* positive nuclei with parvalbumin in the CA3 layer. F) Colocalization of parvalbumin positive neurons with *c-fos* in the CA3 layer. Animal numbers were 4 for controls, n=3 for PTZ 20, n=2 for PTZ 40, and n=3 for PTZ80. Statistics: * p<.05, ** p<.01, *** p<.001 as compared to controls; # p<.05, ## p<.01 as indicated.